Maternal High-Fat Diet Induces Sex- and Estrous Cycle–Specific Glial Dysregulation in the Peripheral Offspring Retina

Gintare Urbonaite,[1] Patricija Cepauskyte,[1] Neda I. Biliute,[1,2] Guoda Laurinaviciute,[3] Daiva Dabkeviciene,[1] Solveiga Samulėnaitė,[1,4] and Urte Neniskyte[1,5]

[1]Institute of Biosciences, Vilnius University Life Sciences Center, Vilnius, Lithuania
[2]Laboratory of Cognitive and Adaptive Neurosciences (LNCA), University of Strasbourg, Strasbourg, France
[3]Institute of Biomedical Sciences, Faculty of Medicine, Vilnius University, Vilnius, Lithuania
[4]Department of Biological Models, Institute of Biochemistry, Vilnius University Life Sciences Center, Vilnius, Lithuania
[5]VU LSC-EMBL Partnership Institute for Genome Editing Technologies, Vilnius University Life Sciences Center, Vilnius, Lithuania

Correspondence: Urte Neniskyte, VU LSC-EMBL Partnership Institute for Genome Editing Technologies, Life Sciences Center, Vilnius University, Sauletekio al. 7, Vilnius 10257, Lithuania;
urte.neniskyte@gmc.vu.lt.

Received: February 10, 2026
Accepted: July 5, 2026
Published: August 7, 2026

Citation: Urbonaite G, Cepauskyte P, Biliute NI, et al. Maternal high-fat diet induces sex- and estrous cycle–specific glial dysregulation in the peripheral offspring retina. *Invest Ophthalmol Vis Sci.* 2026;67(10):20.
https://doi.org/10.1167/iovs.67.10.20

Purpose. A maternal high-fat diet (mHFD) induces metabolic disturbances that lead to inflammatory responses in the offspring's brain. The retina, as part of the central nervous system, may be similarly affected. This study aimed to determine how mHFD affects microglial and Müller cell activity in the retinas of offspring and assess how these effects depend on sex and the female estrous cycle.

Methods. Female C57Bl/6J mice were fed a control diet (10% fat) or a high-fat diet (60% fat) from weaning to lactation. The offspring were weaned to a normal rodent diet. Retinal structure and glial cells were assessed using immunohistochemical labeling of retinal ganglion cells, Müller glia, and phagocytic and inflammatory markers. Observed retinal changes in female offspring were correlated with the estrous cycle stages.

Results. mHFD induced subtle retinal structural changes and sex-specific alterations in glial cells of offspring peripheral retina. Male offspring exhibited a reduced microglial area, accompanied by an increased lysosomal/phagolysosomal profile, whereas females showed the opposite pattern. Under the maternal control diet, the microglial area and its phagocytic and metabolic immunoreactivity fluctuated with the female estrous cycle, whereas mHFD diminished the differences between phases. Additionally, mHFD reduced Müller glial immunoreactivity in females, suggesting altered glial communication.

Conclusions. Our findings demonstrate that mHFD has a sex-specific effect on the offspring's peripheral retina, affecting the response of retinal microglia to female reproductive hormones.

Keywords: maternal high-fat diet, retinal inflammation, retinal glia, microglia, estrous cycle

A high-fat diet (HFD) is one of the primary factors contributing to the development of metabolic disorders, including obesity, glucose intolerance, insulin resistance, and chronic inflammation.[1–4] There is growing evidence that these alterations could not only affect peripheral tissues but also extend to the central nervous system.[5,6] In particular, the retina is one of the most metabolically active neural tissues, relying heavily on fatty acid stores as an energy source. Alterations in nutrient supply to the retina can drive pathological changes, suggesting that metabolic disturbances induced by HFD may also adversely affect retinal health.[7]

Although the results vary, evidence from animal studies suggests that HFD may promote retinal inflammation, oxidative stress, and neurodegenerative changes.[8–10] One of the first cells to respond to stress in the retina is the microglia. HFD can disrupt microglial function, leading to an increase in microglial soma size, a morphological shift from a ramified to an amoeboid (activated) state, and an overall increase in microglial area and cell number.[11,12] Some studies link increased microglial density and metabolic dysfunction to HFD-induced inflammation and oxidative stress in the retina, enhancing microglial phagocytosis.[10,13]

Another important type of glia that maintains retinal homeostasis and provides both metabolic and structural support to neurons is Müller cells. This specialized columnar glia spans the entire thickness of the retina.[14] In response to retinal injury or inflammatory activation, Müller cells exhibit increased expression of glial fibrillary acidic protein (GFAP), a marker widely used to indicate gliosis.[15] There is evidence that Müller cells can signal to microglia through the extracellular release of glutamate and adenosine triphos-

Copyright 2026 The Authors

This work is licensed under a Creative Commons Attribution 4.0 International License.

Downloaded from iovs.arvojournals.org on 11/03/2026

Investigative Ophthalmology & Visual Science

phate (ATP), thereby conveying changes in neuronal activity. In return, activated microglia secrete pro-inflammatory cytokines (e.g., IL-1β, IL-6), which modulate Müller cell gliosis.[15,16] Typically, microglial activation corresponds with increased Müller cell reactivity; however, in certain pathological conditions, a reduction in Müller glial activation can be observed.[17]

Increasing evidence suggests that glial responses are sex dependent. Animal studies have shown that microglial activation, density, and morphology, as well as Müller cell gliosis, differ between males and females, both during development and in response to inflammation.[18,19] The underlying mechanisms driving these sex-specific differences are likely linked to the influence of sex hormones. Studies suggest that testosterone in males exerts anti-inflammatory effects, attenuating microglial activation and reducing the secretion of pro-inflammatory cytokines.[20] By contrast, in females, the inflammatory response is modulated by hormonal fluctuations across the estrous cycle and can induce changes in inflammatory processes, both in the body and in the brain.[21–23] Although estradiol predominantly exerts anti-inflammatory and neuroprotective effects, it can also enhance microglial phagocytic activity.[23,24] Microglial activity can also be modulated by progesterone, which generally has anti-inflammatory properties and suppresses microglial activation and CD68 expression but, conversely, increases translocator protein (TSPO) protein levels.[25–27]

Collectively, current knowledge indicates that HFD induces inflammation, driving a wide spectrum of structural and functional alterations in the retina. However, studies have focused on the direct effects of HFD on the individual, rather than the influence of a maternal high-fat diet (mHFD) on the retina of their offspring. Meanwhile, many neurodevelopmental studies have shown that the maternal diet can program the metabolic and inflammatory state of the offspring, including the sensitivity of microglia to hormonal signals. For this reason, our study aimed to evaluate the impact of mHFD on the retinal structure of offspring, as well as microglial activation and Müller glia, and whether this effect differs depending on the female estrous cycle stages.

Methods

Animals

C57BL/6J mice were obtained from local Vilnius University Life Sciences Center colonies and were kept under controlled conditions (≥2 mice per cage, 22°C ± 1°C, 12-hour light/dark cycle, food and water ad libitum). Female mice were fed either a control diet (CD) containing 10% kcal from fat (C1090-10 mod; Altromin International, Lage, Germany), or a high-fat diet containing 60% kcal from fat (C1090-60; Altromin International). Of the 16 dams used, eight were assigned to the CD group and eight to the HFD group. Dams were randomly allocated to the dietary groups. Randomization was performed by mixing females from different litters and maintaining equivalent mean body weight (CD, 8.88 ± 1.46*g*; HFD, 8.91 ± 1.42*g*; $P = 0.0033$, two one-sided *t*-tests [TOST]) and median body weight (CD, 8.90*g*; HFD, 8.87*g*) across the experimental groups and home cages. Mice were maintained on these diets from weaning for 10 weeks and during the subsequent pairing, pregnancy, and lactation periods. Maternal metabolic status was evaluated by weekly body weight measurements, followed by glucose and insulin tolerance tests after 10 weeks of diet feeding, before pairing. Female mice were paired with homozygous male *Thy1*::EGFP (JAX:007788; International Mouse Strain Resource [IMSR]), *Cx3cr1*::CreER (JAX:021160; IMSR), or *RC*::LSL-tdTomato (JAX:007905; IMSR) mice on a C57BL/6J background[28] for the fluorescence labeling of neurons and microglia cells. Both the males before pairing and the offspring after weaning were maintained on standard rodent chow (NFM18; Mucedola Settimo Milanese, Italy). The estrous cycle stages were determined by vaginal cytology in female offspring on the day of tissue collection at 22 postnatal weeks; crystal violet–dyed smears were imaged using an ECLIPSE Ti-S microscope (Nikon Corporation, Tokyo, Japan) at 20× magnification. For retinal tissue analysis, we used five or six male offspring and nine to 12 female offspring per each of the maternal control diet (mCD) and mHFD groups. Offspring used for retinal analysis were derived from four to nine independent maternal cages per group (females, $n = 12$ and seven to nine maternal cages; males, $n = 6$ and four maternal cages). Multiple offspring of both sexes ($n = 1$–3 for both males and females) were used from each maternal cage. Sample size was estimated based on previous pilot studies (Cohen's $f = 0.310$), targeting 80% power at $\alpha = 0.05$. Imaging analysis and quantification were performed blinded. The project was approved by the Lithuanian State Food and Veterinary Service (No. G2-139). All animal experiments adhered to the requirements of European Directive 2010/63/EU and the ARVO Statement for the Use of Animals in Ophthalmic and Vision Research.

Retinal Sample Collection

Eyeballs were collected from offspring whose mothers were fed either a CD or an HFD. Animals were anesthetized intraperitoneally with a mixture of 100-mg/kg ketamine and 10-mg/kg xylazine and then transcardially perfused with 0.9% NaCl. Dissected eyeballs were fixed with 4% paraformaldehyde (PFA) for 24 hours at 4°C. After sucrose cryoprotection, fixed eyeballs were embedded in Cryomatrix Embedding Medium (Epredia, Kalamazoo, MI, USA) and snap-frozen at −80°C. Frozen samples were cryosectioned at a thickness of 15 µm using a Cryotome FE & FSE cryostat (Epredia).

Immunostaining

Retinal slices were permeabilized and blocked using 20% normal goat serum (NGS) and 0.4% Triton X-100 in PBS for 2 hours at room temperature with gentle shaking. Subsequently, retinal sections were incubated overnight in 20% NGS and 0.4% Triton X-100 at 4°C with selected primary antibodies, followed by corresponding secondary antibodies (Table) for 2 hours at room temperature. Immunolabeled retinas were stained with 4′,6-diamidino-2-phenylindole (DAPI; 1 µg/mL) and mounted with Mowiol medium (Sigma-Aldrich, St. Louis, MO, USA). Retinal thickness measurement and ganglion cell counting were performed using a TCS SP8 confocal microscope (Leica Microsystems, Wetzlar, Germany) with a 20×/0.75 numerical aperture (NA) objective (0.568 µm/pixel). Anti–ionized calcium-binding adapter molecule1 (Iba1)-marked microglia and anti–GFAP-marked Müller cells were imaged using an EVOS FL Auto Imaging System (Thermo Fisher Scientific, Waltham, MA) with a 20×

Investigative Ophthalmology & Visual Science

Downloaded from iovs.arvojournals.org on 11/03/2026

Table. Antibodies Used in This Study

Type	Antibody	Source (Catalog No.)	RRID	Dilution
Primary antibody	Rabbit anti-Iba1	FUJIFILM Wako Chemicals USA (019-19741)	AB_839504	1:1000
	Mouse anti-RFP (recognizing tdTomato)	Rockland Immunochemicals (200-301-379)	AB_2611063	1:1000
	Rat anti-CD68	Thermo Fisher Scientific (14-0681-82)	AB_2572857	1:200
	Rabbit anti-PBR/TSPO	Abcam (ab109497)	AB_10862345	1:400
	Chicken anti-GFAP	Abcam (ab4674)	AB_304558	1:1000
	Rabbit anti-RBPMS	GeneTex (GTX118619)	AB_10720427	1:1000
Secondary antibody	Goat anti-rabbit Alexa Fluor 594	Thermo Fisher Scientific (A-11012)	AB_2534079	1:500
	Goat anti-mouse Alexa Fluor 647	Thermo Fisher Scientific (A-32733)	AB_2535813	1:500

RRID, Research Resource Identifier; RFP, red fluorescent protein; PBR, peripheral benzodiazepine receptor.

objective (0.45 µm/pixel). Anti-tdTomato, anti-CD68, and anti-TSPO immunolabeled areas were imaged using an IX83 widefield fluorescence microscope (Olympus, Tokyo, Japan) with a 20× objective (0.325 µm/pixel). Images were acquired using identical exposure settings within each immunofluorescence experiment.

Retinal Layer Thickness and Ganglion Cell Count Assessment

To separate retinal layers and count ganglion cells, the slices were immunolabeled with anti–RNA-binding protein with multiple splicing (RBPMS) and stained with DAPI. The thickness of the retinal layers was evaluated by measuring 10 to 15 positions at different locations across the central and peripheral 500-µm retinal segments and calculating the average thickness for each image. Relative retinal thickness was determined according to the following equation:

$$\frac{x \text{ thickness}}{\text{Whole retina thickness}} \times 100\%$$

Ganglion cells labeled with anti-RBPMS were quantified by applying the same threshold and automated particle counting using ImageJ/Fiji (National Institutes of Health, Bethesda, MD, USA). Cell counts were determined within 500-µm-long central and peripheral retinal segments (cells/500 µm).

Microglia and Müller Cell Analysis

The distribution of microglia and Müller cells in retinal segments was evaluated in Iba1- and GFAP-immunolabeled retinal slices, respectively. First, using the ImageJ/Fiji program, each 8-bit grayscale retinal image was cropped into 500-µm-long segments measured from the retinal margin along the outer nuclear layer (ONL), which were defined as peripheral retinal regions. Central retinal regions were defined as 500-µm-long segments surrounding the optic nerve. Due to variability in tissue quality and staining, some samples were excluded from analysis (e.g., damaged sections, incomplete peripheral retinal regions), resulting in estrous stage subgroup sizes of two or three animals per group. Cell area was estimated by processing images: subtracting the background (radius 50), applying a median filter (radius 1) and a Gaussian blur (sigma radius 1), and finally measuring the area of the created masks using ImageJ/Fiji. Thresholding was performed to create binary masks representing positive signals. The threshold was selected manually using representative images from all experimental groups. The lowest value of threshold that maintained specific fluorescence while also excluding background noise was selected and used for all of the images. All images were processed using established identical threshold parameters and regions of interest (ROIs) to ensure reproducibility.

To analyze the microglia area in the central and peripheral retina, microglia cells were marked with anti-Iba1 and processed as described above. The microglia area was determined within the generated binary mask after thresholding. Retinal sections were stained with antibodies against tdTomato (used to genetically label microglia), CD68, and TSPO and analyzed in peripheral retinal segments. Image channels corresponding to individual antibody signals were separated, and each channel was processed as described above. tdTomato and CD68 or tdTomato and TSPO overlay binary masks were generated, and total microglial area, as well as the quantification of anti–CD68- and anti–TSPO-positive microglial areas, were performed. Area fraction (%) was calculated as (positive mask area/ROI area) × 100. For retinal analysis, one eye per animal was used, with four or more sections and images analyzed per animal. Statistical analyses were performed using animal-level averages.

Müller cell area and Müller glial processes lengths were quantified across all retinal layers in the peripheral retina. The lengths of Müller cell processes were determined at five different positions per retinal segment by calculating the ratio of total retinal layer width to the extent of the penetration of the GFAP-positive processes into the layers. The channels were then split, and images were processed as described above. To determine the total GFAP-positive Müller cell area in the peripheral retina of the offspring, the auto local threshold value was applied across all samples (Bernsen method; radius, 5 pixels).

Statistical Analysis

Because offspring from two dams housed in the same cage could not be reliably assigned to individual litters after birth, and the number of mice obtained from each maternal cage was limited, animal ID was used as the primary experimental unit in the statistical analysis. To assess differences in area between experimental animal groups, a statistical analysis was performed using a custom Python 3.8 script generated and completed in the Spyder environment via the Anaconda platform. Regarding outlier handling, samples flagged by the mean ± 1.5 SD criterion were additionally assessed for technical quality issues, such as tissue damage, poor staining, or incomplete retinal regions, and they were subsequently excluded if necessary. Then, a nested two-way

Investigative Ophthalmology & Visual Science

Downloaded from iovs.arvojournals.org on 11/03/2026

ANOVA (Factor ~ C[Sex] * C[Diet] + C[ID]:C[Sex_Diet]) was conducted to assess the effects of sex (or estrous cycle stage), maternal diet, and their interaction on the area of retinal biomarkers, including a nested random factor (animal ID) to account for within-subject variation. Pairwise comparisons were performed using Tukey's post hoc test to identify specific group differences related to sex, diet, or estrous cycle stage.

Results

Maternal Metabolic Status Is Altered by HFD: Effects on Body Mass, Glucose, and Insulin Tolerance

In this study, to investigate how maternal diet-induced metabolic changes affect offspring retina, the mHFD mouse model was implemented (Fig. 1A). Females receiving the HFD gained significantly more weight after 3 weeks of diet consumption compared to the CD group (Fig. 1B). Metabolic tests indicated that HFD females developed impaired glucose tolerance with elevated blood glucose levels from 30 minutes after glucose injection onward (Fig. 1C). HFD reduced insulin sensitivity, with elevated glucose levels detected at the 40- and 60-minute time points after insulin injection (Fig. 1D).

mHFD Induced Changes in Peripheral Retinal Microglial Immunoreactivity, Depending on the Sex and Estrous Cycle of the Female

In pilot studies, microglial areas were assessed in the central and peripheral retina using Iba1 immunostaining (Supplementary Fig. S1) in samples prepared as presented in Figure 1E. We found no differences in microglial area between groups in the central retina (Supplementary Fig. S1C); however, the effects of sex and diet were observed in the peripheral retina (Supplementary Fig. S1D). Under mCD, the microglia area in the retinas of males was larger than that of females, consistent with the known physiological effect of sex hormones.[29] However, the mHFD appears to be associated with a sex-specific remodeling of the microglial profile, with a decrease in the male microglial area and an increase in the female microglial area (Supplementary Fig. S1D).

Based on the significant changes observed specifically in the peripheral retina, further detailed analyses were conducted in this retinal area. Using the *Cx3cr1*::tdTomato mouse, in which microglial cells are genetically labeled by tdTomato red fluorescent protein, revealed a similar significant interaction between sex and maternal diet. We found that mHFD significantly decreased the area of tdTomato^{+} microglia in males compared to the mCD group but increased this area in females (Fig. 2B). In this experi-

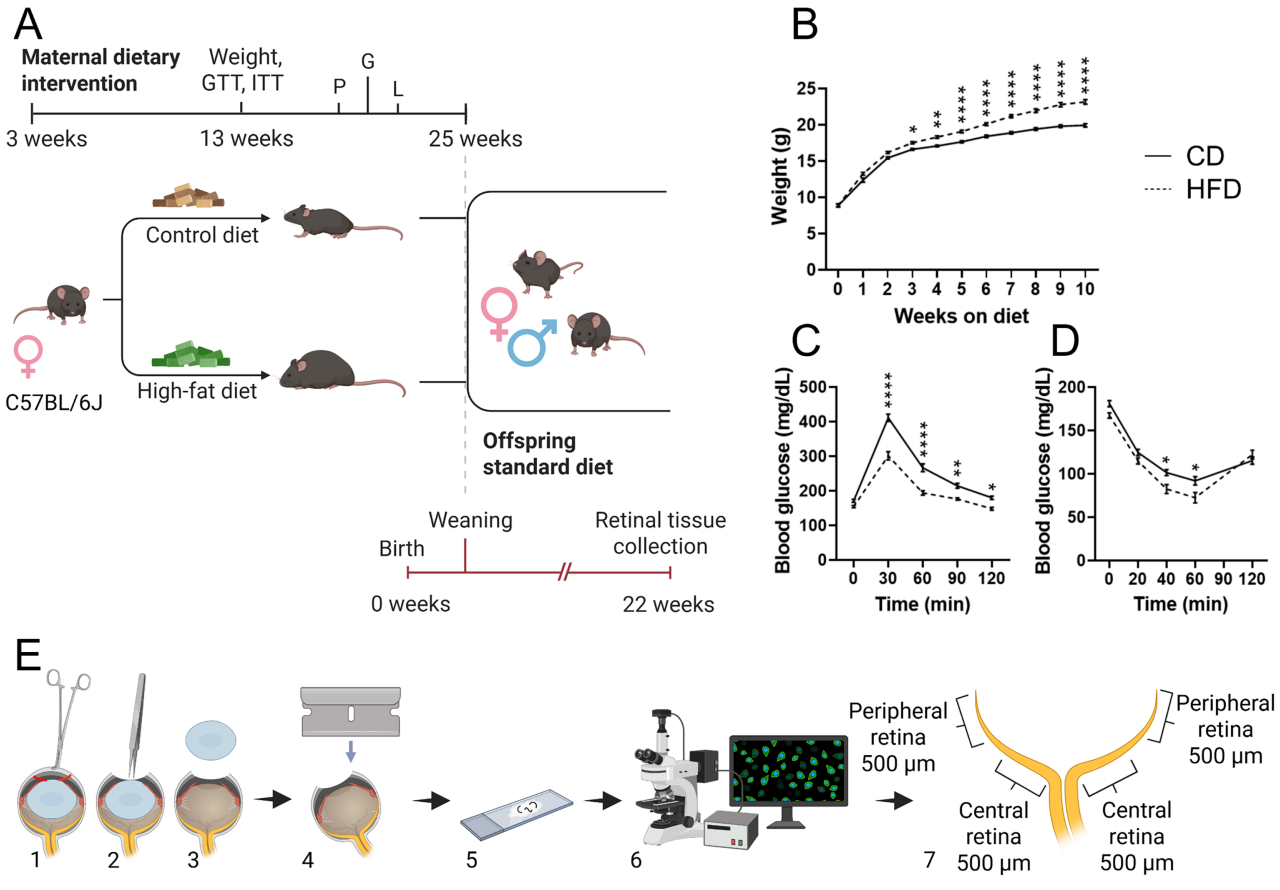

Figure 1. Experimental design and retinal tissue collection workflow. (**A**) Schematic representation of the mHFD mouse model and offspring development timeline. (**B**) Maternal weight. (**C**) Glucose tolerance test. (**D**) Insulin tolerance test. (**E**) Workflow of offspring eyeball dissection, preparation, retinal tissue collection, and fluorescence imaging. P, pregnancy; G, gestation; L, lactation.

Investigative Ophthalmology & Visual Science

Downloaded from iovs.arvojournals.org on 11/03/2026

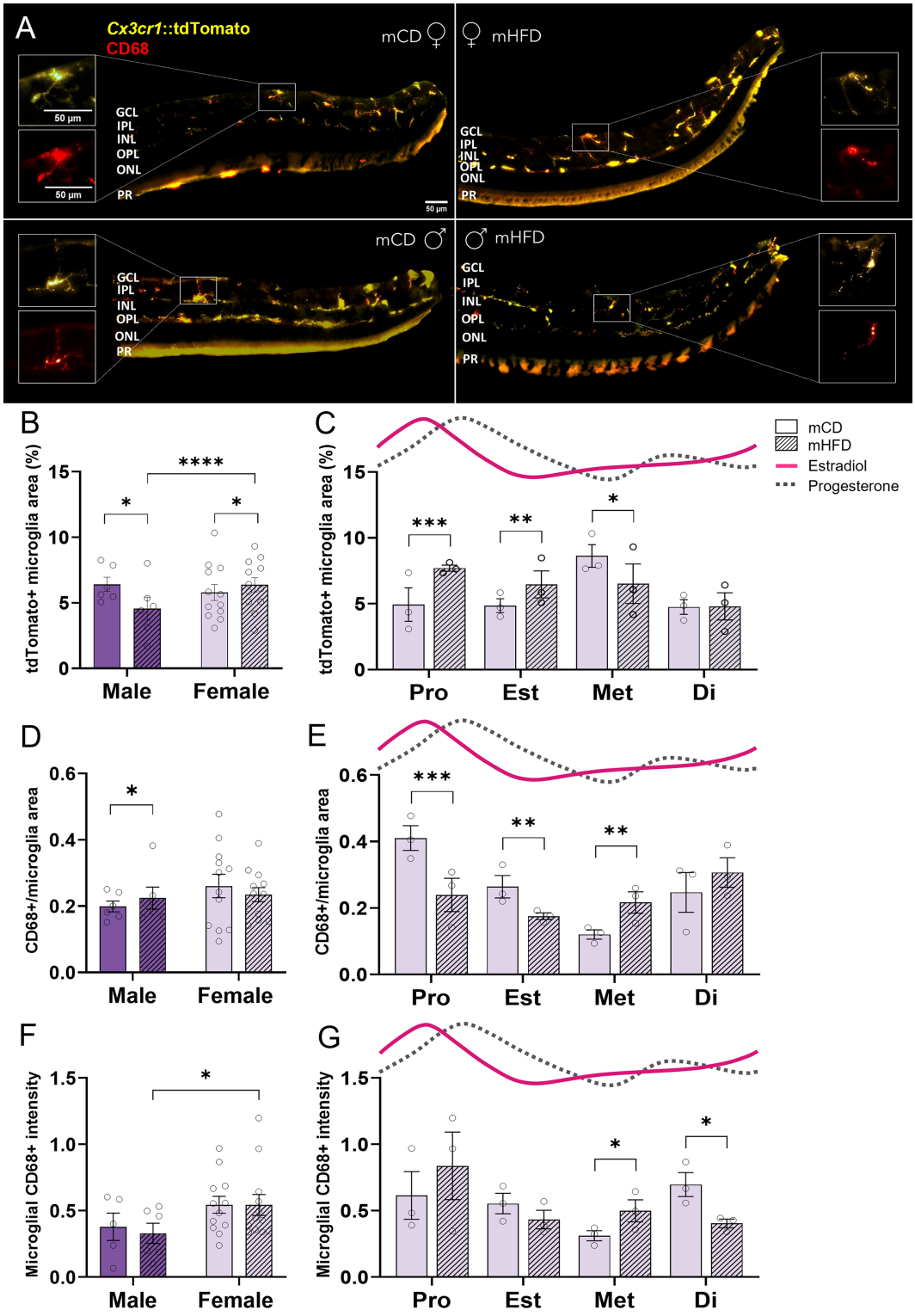

Figure 2. The effects of mHFD on microglia and microglial CD68 of the offspring's peripheral retina. (**A**) Representative confocal images of tdTomato-positive microglia (*Cx3cr1*::tdTomato, *yellow*) and microglial CD68 immunoreactivity (*red*) in peripheral retinal sections from female (♀) and male (♂) offspring of dams who were fed either a control diet (mCD) or a high-fat diet (mHFD). GCL, ganglion cell layer; IPL, inner plexiform layer; INL, inner nuclear layer; OPL, outer plexiform layer; ONL, outer nuclear layer; PR, photoreceptor layer. *Scale bar*: 50 µm. (**B**, **C**) tdTomato$^+$ microglia area fraction (%) by sex (**B**) and by female estrous cycle (**C**). Pro, proestrus; Est, estrus; Met, metestrus; Di, diestrus stages. The *solid line* indicates estradiol; *dashed line*, progesterone. Figure is based on Miller and Takahashi.[30] (**D**, **E**) CD68$^+$/microglia area fraction (%) in the peripheral retina of the offspring by sex (**D**) and by female offspring estrous cycle (**E**). (**F**, **G**) Offspring microglial CD68$^+$ intensity by sex (**F**) and by female offspring estrous cycle stages (**G**). Mean ± SEM (n = 6 males and 3 females per estrous stage per group; total n = 12 per group). P values were assessed using nested two-way ANOVA with Tukey's post hoc tests. *P < 0.05, **P < 0.01, ***P < 0.001, ****P < 0.0001.

Investigative Ophthalmology & Visual Science

Downloaded from iovs.arvojournals.org on 11/03/2026

ment, mHFD revealed sex-specific changes in the microglial profile that were not evident in the control diet group.

To address the fluctuation of female sex hormones, females were further separated by estrous cycle based on cytological images of vaginal smears (Supplementary Fig. S2). Under physiological conditions (mCD group), the area of tdTomato$^+$ microglia varied depending on the phase of the estrous cycle: It was lower during proestrus and estrus (highest estradiol and progesterone levels), highest in the metestrus phase (lowest estradiol and progesterone levels), and then decreased again (Fig. 2C). Although hormone levels were not directly measured in this study, fluctuations in estradiol and progesterone concentrations across the estrous cycle are well documented in the literature.[30] Importantly, we determined that mHFD disrupted these cyclical microglial dynamics, reducing the differences of microglial area between the phases (Fig. 2C). In addition, we found that mHFD significantly increased the area of tdTomato$^+$ microglia during proestrus and estrus phases and decreased them during the metestrus phase (Fig. 2C). These results suggest that mHFD may alter microglia response to estrogen or progesterone signals during the estrous cycle.

One of the main functions of microglia is phagocytosis. Microglial phagocytic activity can be assessed using the CD68 glycoprotein expressed on lysosomal membranes.[31,32] Our analysis of the CD68$^+$ area of microglia revealed sex- and estrous cycle–dependent changes in microglial lysosomal/phagolysosomal profiles. As shown in Figure 2D, we found that mHFD significantly increased the area of microglial CD68 in males, indicating increased CD68 immunoreactivity and suggesting altered lysosomal/phagolysosomal activity. In females, by contrast, the CD68$^+$ area did not increase overall, but a clear dependency on the phases of the estrous cycle was observed (Fig. 2E). After the evaluation of individual phases (Fig. 2E), we determined that the area of microglial CD68 in mCD females was the highest in the proestrus phase and the lowest during metestrus. Strikingly, we found that mHFD disrupted this cyclical pattern, reducing the areas of CD68 in the proestrus and estrus phases but increasing the area in the metestrus phase (Fig. 2E). This suggests that mHFD reverses the normal direction of the estrous cycle pattern, suggesting altered microglial lysosomal/phagolysosomal activity at high estradiol and progesterone levels with an increase when these hormones are reduced.

When we assessed the intensity of the microglial CD68$^+$ signal, we found that the total CD68 intensity was higher in females than in males, and it fluctuated during the estrus cycle in response to varying hormone levels (Figs. 2F, 2G). Meanwhile, mHFD distorted this profile, as the CD68 intensity increased in metestrus and decreased in diestrus (Fig. 2G), suggesting an altered microglial response to hormonal changes.

Because the changes in microglial activity may affect retinal cell viability and tissue integrity,[33–35] we assessed the thickness of the total retina and its separate layers (Supplementary Fig. S3). In mCD females, the total central retinal thickness was greater than in males, but mHFD significantly reduced it, even though this effect was not observed in males (Supplementary Fig. S3C). After the evaluation of individual central layers, we found that in males mHFD thinned the photoreceptor (PR) layer but increased the thickness of the ONL (Supplementary Fig. S3D). In the peripheral retina, mHFD increased total retinal thickness exclusively in females (Supplementary Fig. S3E). In males, mHFD changed the thickness of individual peripheral layers, reducing the PR but increasing the thickness of the ONL and outer plexiform layer (OPL) (Supplementary Fig. S3F). Meanwhile, we did not find any effect of mHFD on the number of retinal ganglion cells in either the central or peripheral parts of the retina of either sex (Supplementary Figs. S3G, S3H). Because the effects of mHFD on microglial activity showed clear sex and hormonal cycle differences, we aimed to determine whether these changes were also reflected in other markers of microglial immunoreactivity.

mHFD Altered Microglial TSPO Expression in a Sex- and Estrous Cycle–Dependent Manner

The maintenance of microglial function requires high levels of energy, and mitochondria play a central role in supporting these processes.[36] TSPO, located in the outer mitochondrial membrane, is upregulated during retinal inflammation and serves as a marker of microglial activation.[37,38] We determined that, although the microglial TSPO area in the peripheral retina was similar in both sexes of the mCD offspring, the exposure to mHFD induced significant differences in microglial TSPO between the sexes (Fig. 3B). These results are consistent with previously described differences in microglial area (Fig. 2B), indicating that both the inflammatory response of microglia and its regulation of microglial reactivity to maternal metabolic state may be sex specific.

We then evaluated the retinas of females according to the phases of the estrous cycle (Fig. 3C), finding that the microglial TSPO area in the mCD group fluctuated cyclically, varying across estrous cycle stages. In contrast, we found that mHFD disrupted this cyclical pattern, abolishing the differences among phases and causing an increase in microglial TSPO during the diestrus phase. This suggests that mHFD may alter the hormonal regulation of TSPO expression in microglia, potentially associated with increased inflammatory and metabolic signaling at phases when this activity should be physiologically suppressed. The observed changes in microglial immunoreactivity suggest that mHFD may induce a broader glial response in the retina.

Changes in Müller Glial Reactivity After mHFD Exposure

To determine whether these microglial changes were accompanied by alterations in other retinal glial populations, we next assessed Müller glial immunoreactivity. Using GFAP immunohistochemical labeling, we found that mHFD tended to reduce the area of Müller glia, but a statistically significant reduction was only observed in females (Fig. 4B). Furthermore, we determined that mHFD caused shortening of the processes, also exclusively in females (Fig. 4C). These results indicate that mHFD is associated with reduced Müller glial GFAP immunoreactivity and may affect the structural integrity of retinal glia in a sex-specific manner. The reduction in Müller glia area and shortening of processes following mHFD suggest reduced glial reactivity. As an increase in microglial area and activity was observed simultaneously, these results suggest that mHFD induces an imbalance in retinal glial response, with microglia showing increased immunoreactivity and Müller glia showing reduced GFAP expression. Such an imbalance in glial interregulation may contribute to a more pro-inflammatory microenvironment

Investigative Ophthalmology & Visual Science

Downloaded from iovs.arvojournals.org on 11/03/2026

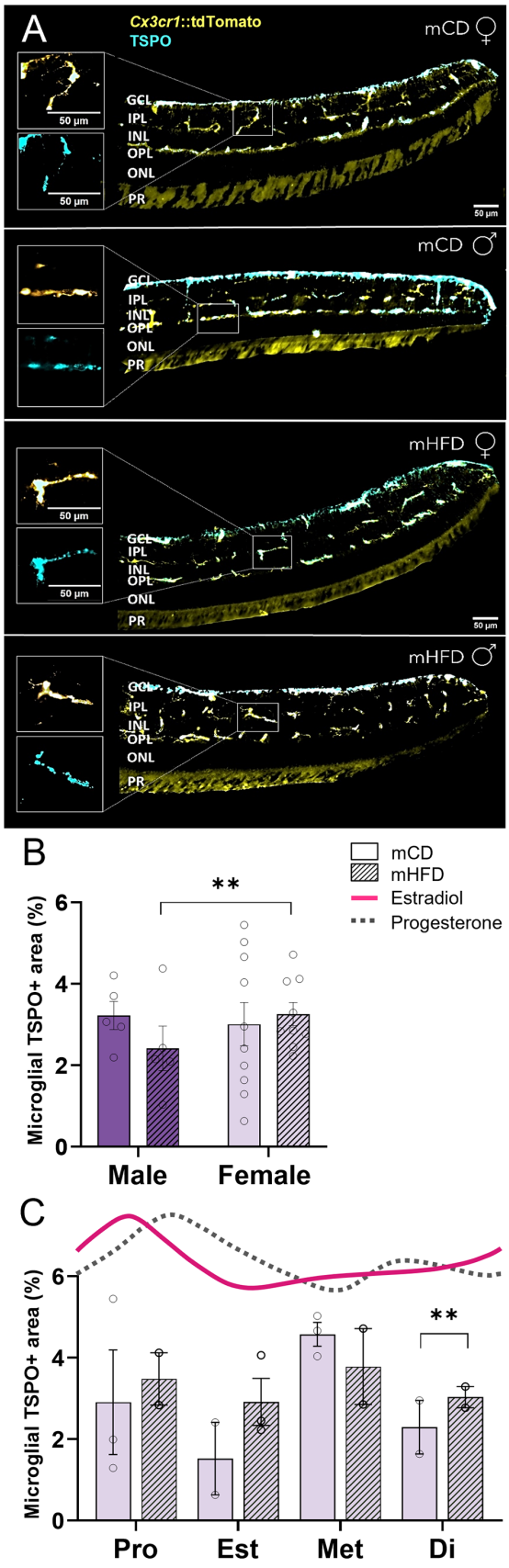

Figure 3. The effects of mHFD on microglial TSPO in the peripheral retina of the offspring. (**A**) Representative confocal images of tdTomato-positive microglia (*Cx3cr1*::tdTomato, *yellow*) and microglial TSPO immunoreactivity (*cyan*) in the peripheral retinal sections from female (♀) and male (♂) offspring of dams who were fed either a control diet (mCD) or a high-fat diet (mHFD). *Scale bar*: 50 µm. (**B**, **C**) Microglial TSPO area fraction (%) in the peripheral retina of the offspring by sex (**B**) and by female offspring estrous cycle (**C**). Pro, proestrus; Est, estrus; Met, metestrus; Di, diestrus. The *solid line* indicates estradiol; *dashed line*, progesterone. Figure is based on Miller and Takahashi.[30] Mean ± SEM ($n = 5$ males and 2 or 3 females per estrous stage per group; total $n = 9$ or 10 per group). P values were assessed using nested two-way ANOVA with Tukey's post hoc tests. *$P < 0.05$, **$P < 0.01$, ***$P < 0.001$, ****$P < 0.0001$.

in the retina, potentially affecting retinal resistance to metabolic stress.

Discussion

This study demonstrates that mHFD is associated with retinal glial function in a sex- and hormone-dependent manner, affecting both microglial activation and Müller glial immunoreactivity. Our data are broadly consistent with previous studies showing that HFD is associated with inflammatory and degenerative changes in the retina. Retinal thinning, layer degeneration, and cell loss have been described in HFD models,[33–35] although some authors did not find significant differences between HFD and CD-fed mice.[9,39] Previous studies have shown that HFD may increase oxidative stress and inflammatory signaling. These findings suggest that diet-related metabolic stress may increase retinal vulnerability, particularly in susceptible models or under additional stress conditions.[40,41] In our study, we found that mHFD is associated with minor structural alterations in the total offspring retina and in its separate layers in both sexes (Supplementary Fig. S3). These results suggest that mHFD did not cause overt retinal degeneration in the offspring.

In most studies, it has been reported that HFD increased inflammation in the CNS, including in the retina, together with an increase in microglial activity.[9,10] Our results confirmed that the HFD-induced inflammatory response is reflected in the offspring. We found that the microglial cell area was altered in the peripheral retina (Supplementary Fig. S1), suggesting that the periphery may be more susceptible to metabolic and inflammatory stress. In this region, reduced vascular density and longer diffusion distances limit metabolic support, which may increase susceptibility to inflammatory activation.[42]

It is known that mHFD influences offspring brain development through inflammatory pathways, often in a sex-dependent manner. Male offspring typically show stronger pro-inflammatory microglial activation, whereas females show more variable or opposite responses.[43,44] However, sex-specific effects of mHFD on offspring retinal microglia have not been previously described. Our findings revealed that mHFD decreased the area of microglia in males but increased it in females (Fig. 2B), suggesting opposite regulation of retinal microglia between sexes that may be influenced by hormonal modulation.

Under normal conditions, we found that the area of microglia varied across the estrous cycle (Fig. 2C). This pattern aligns with studies in the hippocampus and hypothalamus, which show that high ovarian hormone levels suppress microglial activation, whereas their withdrawal promotes a more reactive morphology and increased cytokine expression.[19,45] Our results revealed that mHFD

Investigative Ophthalmology & Visual Science

Downloaded from iovs.arvojournals.org on 11/03/2026

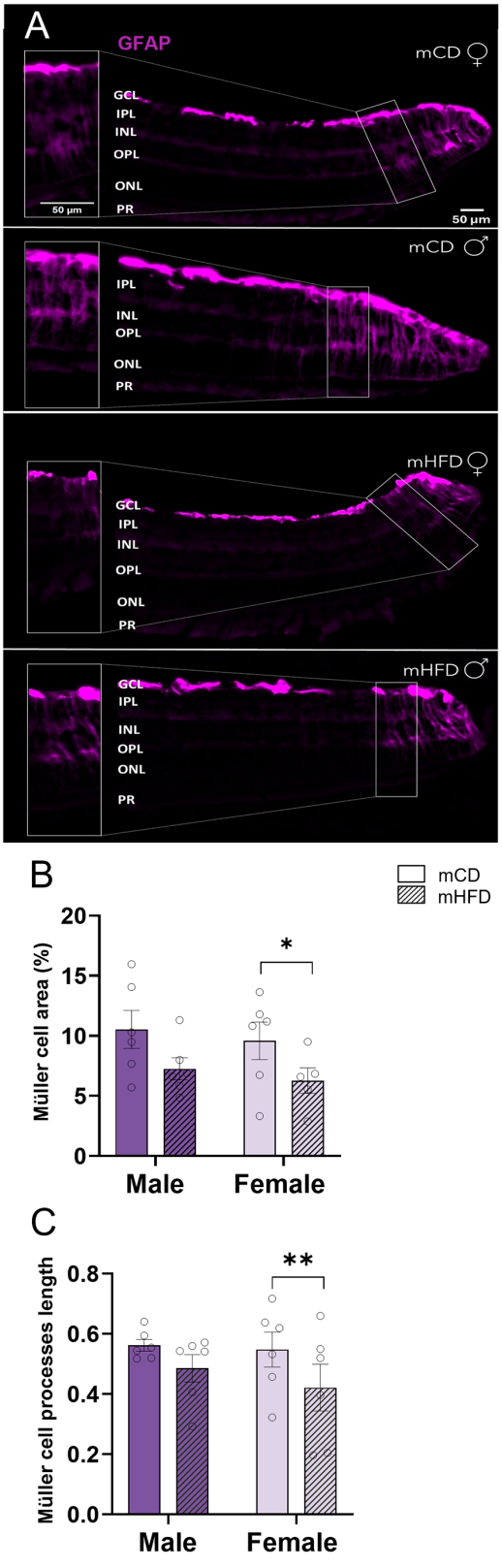

Figure 4. The effects of mHFD on Müller cells in peripheral retina of the offspring. (**A**) Representative confocal images of GFAP-positive (*magenta*) in sections of the peripheral retina from female (♀) and male (♂) offspring of dams who were fed either a control diet (mCD) or a high-fat diet (mHFD). *Scale bar*: 50 µm. (**B**) Müller cell area fraction (%) in the peripheral retina of the offspring. (**C**) Müller cell process length in the peripheral retina of the offspring. Mean ± SEM (n = 5 or 6 per group). P values were assessed using nested two-way ANOVA with Tukey's post hoc tests. *$P < 0.05$, **$P < 0.01$, ***$P < 0.001$, ****$P < 0.0001$.

disturbed the normal pattern in the female offspring: The differences between cycle phases were reduced, and the microglial area increased during specific estrous cycle stages. Together, our data suggest that maternal diet may disrupt the relationship between estrous cycle stages and immune regulation in the retina, potentially increasing vulnerability to inflammation when hormonal protection is reduced.

In addition to the changes in the microglia area, we observed alterations in other markers of microglial activation. Although mHFD reduced the microglial area in males, the area of phagolysosomal marker CD68 within microglia increased (Fig. 2D), suggesting enhanced lysosomal or phagocytic activity. This suggests that mHFD promotes a more activated or metabolically engaged microglial phenotype even when overall microglial coverage is reduced. This pattern is consistent with findings from obesity and diabetes models, which show elevated lysosomal markers in microglia exposed to metabolic stress.[13] In mCD females, CD68 area within microglia changed dynamically across the estrous cycle (Fig. 2E), a pattern consistent with reports that ovarian hormones enhance microglial phagocytic capacity while limiting pro-inflammatory signaling.[24] However, mHFD disrupted the estrous cycle pattern, flattening the differences between phases. To better assess microglial activation, we also analyzed CD68 intensity (Figs. 2F, 2G), which reflects its expression level. Although the CD68 area decreased in proestrus, CD68 intensity tended to increase, suggesting a potential increase in lysosomal CD68 content per microglial cell. Together, these results suggest that mHFD is associated with alterations in microglial lysosomal marker profiles, indicating changes in microglial state but hormonal unresponsiveness.

In addition to the CD68 findings, we examined TSPO to further evaluate how mHFD affects microglial mitochondrial function. Under physiological conditions, microglial TSPO area followed the pattern across estrous cycle stages (Fig. 3C), showing mild fluctuations across the estrous cycle. Our results revealed that, after mHFD exposure, this pattern was lost, suggesting altered relationships between estrous cycle stage and TSPO expression in microglia. However, due to sample exclusion related to tissue quality and staining, some estrous stage subgroups in the TSPO analysis included only two or three animals per group; therefore, the results should be interpreted cautiously. The stronger TSPO response in females also supports a sex-dependent sensitivity of retinal microglia (Fig. 3B), which aligns with previous studies that have shown that obesity can alter microglial energy metabolism and inflammatory signaling in a sex-specific manner.[46]

Together, the changes in CD68 and TSPO indicate that mHFD promotes a more persistent microglial immunoreactive profile with reduced variation across estrous cycle stages. Interestingly, we found that this increased microglial immunoreactivity was accompanied by a reduction in Müller cell area and process length in females (Figs. 4B, 4C), suggesting suppressed Müller glial profiles. Because Müller cells play a key role in supporting neurons and communicating with microglia through ATP, glutamate, and cytokine signaling,[15,16] their reduced activation may weaken retinal homeostasis. Similar patterns, where increased microglial activity coincides with diminished GFAP expression, have been reported in neurodegenerative disease models.[17,47] Thus, mHFD may influence the intracellular interactions between microglia and Müller cells, but further molecular investigation is needed.

Investigative Ophthalmology & Visual Science

Downloaded from iovs.arvojournals.org on 11/03/2026

Conclusions

This study demonstrates that mHFD is associated with long-term, sex- and hormone-dependent changes in glial profiles of the offspring retina. These effects primarily occur in the peripheral retina and precede overt neurodegeneration, suggesting that glial dysregulation is an early event in retinal stress. The strength of this work lies in the combined analysis of multiple glial markers (dTomato/Iba1, CD68, TSPO, and GFAP), the inclusion of both sexes and estrous cycle phases, and regional evaluation across the retina, which together provide a comprehensive view of glial diversity and plasticity. However, the functional analyses, such as electrophysiology or visual behavior, were beyond the scope of this work. Furthermore, the imaging approach used in the study only supported the overall evaluation of microglial area, without the possibility to explore the underlying reason for such change, such as alterations in soma size or cell count, as well as ramification complexity. Therefore, future studies are necessary to further elucidate the functional and morphological microglial profile. Future studies should address these aspects and examine whether modulation of microglial metabolism or hormone signaling can restore retinal homeostasis and reduce vulnerability to metabolic stress.

Acknowledgments

The authors thank Igoris Nagula, for help with immunohistochemical labeling of retinal samples; Viktorija Kralikiene, for technical work with animals; and Dovydas Gabrielaitis, Lina Saveikyte, and Ugne Kuliesiute, for their assistance with the technical setups for microscopy and image analysis.

Supported by the Science Promotion Fund of Vilnius University (MSF-JM-4/2021); Research Council of Lithuania (LMTLT) and ERA-NET NEURON Joint Transnational Call (S-NEURON-25-1); and Research Council of Lithuania (LMTLT) under the University Excellence Initiatives of the Ministry of Education, Science and Sports of the Republic of Lithuania (Measure No. 12-001-01-01-01, Improving the Research and Study Environment, S-A-UEI-23-10).

When creating Python scripts for statistical analysis, the authors used GPT 4o, GPT 5.1, and Grammarly 1.142.1.0 to improve language and grammar. After using these tools, the authors reviewed and edited the content.

Author Contributions: Conceptualization: U.N.; Methodology: G.U., G.L., and U.N.; Software: G.U., P.C., and N.I.B.; Formal analysis: G.U., P.C., N.I.B., and D.D.; Investigation: G.U., P.C., and N.I.B.; Data curation: G.U. and U.N.; Writing–original draft: G.U. and P.C.; Writing–review and editing: G.U., P.C., S.S., and U.N.; Visualization: G.U. and P.C.; Supervision: U.N.; Funding acquisition: G.U. and U.N.

Disclosure: **G. Urbonaite**, None; **P. Cepauskyte**, None; **N.I. Biliute**, None; **G. Laurinaviciute**, None; **D. Dabkeviciene**, None; **S. Samulėnaitė**, None; **U. Neniskyte**, None

References

1. Almeida-Suhett CP, Graham A, Chen Y, Deuster P. Behavioral changes in male mice fed a high-fat diet are associated with IL-1β expression in specific brain regions. *Physiol Behav*. 2017;169:130–140.
2. Ellenbroek JH, Töns HA, de Graaf N, et al. Topologically heterogeneous beta cell adaptation in response to high-fat diet in mice. *PLoS One*. 2013;8(2):e56922.
3. Lee YS, Li P, Huh JY, et al. Inflammation is necessary for long-term but not short-term high-fat diet-induced insulin resistance. *Diabetes*. 2011;60(10):2474–2483.
4. Wu Y, Wu T, Wu J, et al. Chronic inflammation exacerbates glucose metabolism disorders in C57BL/6J mice fed with high-fat diet. *J Endocrinol*. 2013;219(3):195–204.
5. Duan Y, Zeng L, Zheng C, et al. Inflammatory links between high fat diets and diseases. *Front Immunol*. 2018;9:02649.
6. Guillemot-Legris O, Masquelier J, Everard A, Cani PD, Alhouayek M, Muccioli GG. High-fat diet feeding differentially affects the development of inflammation in the central nervous system. *J Neuroinflammation*. 2016;13(1):206.
7. Clarkson-Townsend DA, Douglass AJ, Singh A, Allen RS, Uwaifo IN, Pardue MT. Impacts of high fat diet on ocular outcomes in rodent models of visual disease. *Exp Eye Res*. 2021;204:108440.
8. Mohamed IN, Hafez SS, Fairaq A, Ergul A, Imig JD, El-Remessy AB. Thioredoxin-interacting protein is required for endothelial NLRP3 inflammasome activation and cell death in a rat model of high-fat diet. *Diabetologia*. 2014;57(2):413–423.
9. Atawia RT, Bunch KL, Fouda AY, et al. Role of arginase 2 in murine retinopathy associated with western diet-induced obesity. *J Clin Med*. 2020;9(2):317.
10. Lee JJ, Wang PW, Yang IH, et al. High-fat diet induces Toll-like receptor 4-dependent macrophage/microglial cell activation and retinal impairment. *Invest Ophthalmol Vis Sci*. 2015;56(5):3041–3050.
11. Ceasrine AM, Bilbo SD. Dietary fat: a potent microglial influencer. *Trends Endocrinol Metab*. 2022;33(3):196–205.
12. Mendes NF, Kim YB, Velloso LA, Araújo EP. Hypothalamic microglial activation in obesity: a mini-review. *Front Neurosci*. 2018;12:846.
13. Kutsyr O, Noailles A, Martínez-Gil N, et al. Short-term high-fat feeding exacerbates degeneration in retinitis pigmentosa by promoting retinal oxidative stress and inflammation. *Proc Natl Acad Sci USA*. 2021;118(43):e2100566118.
14. Devoldere J, Peynshaert K, De Smedt SC, Remaut K. Müller cells as a target for retinal therapy. *Drug Discov Today*. 2019;24(8):1483–1498.
15. Bringmann A, Pannicke T, Grosche J, et al. Müller cells in the healthy and diseased retina. *Prog Retin Eye Res*. 2006;25(4):397–424.
16. Wang M, Wong WT. Microglia–Müller cell interactions in the retina. In: Ash JD, Grimm C, Hollyfield JG, Anderson RE, LaVail MM, Bowes Rickman C, eds. *Retinal Degenerative Diseases*. Berlin: Springer Nature; 2014:333–338.
17. Xu QA, Boerkoel P, Hirsch-Reinshagen V, et al. Müller cell degeneration and microglial dysfunction in the Alzheimer's retina. *Acta Neuropathol Commun*. 2022;10:145.
18. Hanamsagar R, Alter MD, Block CS, Sullivan H, Bolton JL, Bilbo SD. Generation of a microglial developmental index in mice and in humans reveals a sex difference in maturation and immune reactivity. *Glia*. 2017;65(9):1504–1520.
19. Schwarz JM, Sholar PW, Bilbo SD. Sex differences in microglial colonization of the developing rat brain. *J Neurochem*. 2012;120(6):948–963.
20. O'Connor JL, Nissen JC. The pathological activation of microglia is modulated by sexually dimorphic pathways. *Int J Mol Sci*. 2023;24(5):4739.
21. Ajayi AF, Akhigbe RE. Staging of the estrous cycle and induction of estrus in experimental rodents: an update. *Fertil Res Pract*. 2020;6:5.
22. Sharma C, Venkatappa V, Jayamma Y, Inamdar L. Estrous cycle in rodents: phases, characteristics and neuroendocrine regulation. *J Sci*. 2020;51:40–53.
23. Straub RH. The complex role of estrogens in inflammation. *Endocr Rev*. 2007;28(5):521–574.

Investigative Ophthalmology & Visual Science

Downloaded from iovs.arvojournals.org on 11/03/2026

24. Loiola RA, Wickstead ES, Solito E, McArthur S. Estrogen promotes pro-resolving microglial behavior and phagocytic cell clearance through the actions of annexin A1. *Front Endocrinol (Lausanne)*. 2019;10:420.
25. Benlloch-Navarro S, Trachsel-Moncho L, Fernández-Carbonell Á, et al. Progesterone anti-inflammatory properties in hereditary retinal degeneration. *J Steroid Biochem Mol Biol*. 2019;189:291–301.
26. Coronel MF, Sánchez Granel ML, Raggio MC, et al. Temporal changes in the expression of the translocator protein TSPO and the steroidogenic enzyme 5α-reductase in the dorsal spinal cord of animals with neuropathic pain: Effects of progesterone administration. *Neurosci Lett*. 2016;624:23–28.
27. Wang J, Zhao Y, Liu C, Jiang C, Zhao C, Zhu Z. Progesterone inhibits inflammatory response pathways after permanent middle cerebral artery occlusion in rats. *Mol Med Rep*. 2011;4(2):319–324.
28. Weinhard L, di Bartolomei G, Bolasco G, et al. Microglia remodel synapses by presynaptic trogocytosis and spine head filopodia induction. *Nat Commun*. 2018;9(1):1228.
29. Yanguas-Casás N. Physiological sex differences in microglia and their relevance in neurological disorders. *Neuroimmunol Neuroinflamm*. 2020;7(1):13–22.
30. Miller BH, Takahashi JS. Central circadian control of female reproductive function. *Front Endocrinol (Lausanne)*. 2014;4:195.
31. Chistiakov DA, Killingsworth MC, Myasoedova VA, Orekhov AN, Bobryshev YV. CD68/macrosialin: not just a histochemical marker. *Lab Invest*. 2017;97(1):4–13.
32. Hendrickx DAE, van Eden CG, Schuurman KG, Hamann J, Huitinga I. Staining of HLA-DR, Iba1 and CD68 in human microglia reveals partially overlapping expression depending on cellular morphology and pathology. *J Neuroimmunol*. 2017;309:12–22.
33. Hammoum I, Mbarek S, Dellaa A, et al. Study of retinal alterations in a high fat diet-induced type II diabetes rodent: *Meriones shawi*. *Acta Histochem*. 2017;119(1):1–9.
34. Marçal AC, Leonelli M, Fiamoncini J, et al. Diet-induced obesity impairs AKT signalling in the retina and causes retinal degeneration. *Cell Biochem Funct*. 2013;31(1):65–74.
35. Zhu H, Zhang W, Zhao Y, et al. GSK3β-mediated tau hyperphosphorylation triggers diabetic retinal neurodegeneration by disrupting synaptic and mitochondrial functions. *Mol Neurodegener*. 2018;13(1):62.
36. Aldana BI. Microglia-specific metabolic changes in neurodegeneration. *J Mol Biol*. 2019;431(9):1830–1842.
37. Hector M, Langmann T, Wolf A. Translocator protein (18 kDa) (TSPO) in the retina and implications for ocular diseases. *Prog Retin Eye Res*. 2024;100:101249.
38. Selvaraj V, Stocco DM, Tu LN. Minireview: Translocator protein (TSPO) and steroidogenesis: a reappraisal. *Mol Endocrinol*. 2015;29(4):490–501.
39. Chang RCA, Shi L, Huang CCY, et al. High-fat diet-induced retinal dysfunction. *Invest Ophthalmol Vis Sci*. 2015;56(4):2367–2380.
40. Pillar S, Moisseiev E, Sokolovska J, Grzybowski A. Recent developments in diabetic retinal neurodegeneration: a literature review. *J Diabetes Res*. 2020;2020:5728674.
41. Dao D, Xie B, Nadeem U, et al. High-fat diet alters the retinal transcriptome in the absence of gut microbiota. *Cells*. 2021;10(8):2119.
42. Zouache MA. Variability in retinal neuron populations and associated variations in mass transport systems of the retina in health and aging. *Front Aging Neurosci*. 2022;14:778404.
43. Bilbo SD, Tsang V. Enduring consequences of maternal obesity for brain inflammation and behavior of offspring. *FASEB J*. 2010;24(6):2104–2115.
44. Bordeleau M, Comin CH, Fernández de Cossío L, et al. Maternal high-fat diet in mice induces cerebrovascular, microglial and long-term behavioural alterations in offspring. *Commun Biol*. 2022;5(1):26.
45. Sierra A, Gottfried-Blackmore A, Milner TA, McEwen BS, Bulloch K. Steroid hormone receptor expression and function in microglia. *Glia*. 2008;56(6):659–674.
46. Murtaj V, Belloli S, Di Grigoli G, et al. Age and sex influence the neuro-inflammatory response to a peripheral acute LPS challenge. *Front Aging Neurosci*. 2019;11:299.
47. Fernández-Albarral JA, de Hoz R, Matamoros JA, et al. Retinal changes in astrocytes and Müller glia in a mouse model of laser-induced glaucoma: a time-course study. *Biomedicines*. 2022;10(5):5.

Investigative Ophthalmology & Visual Science

Downloaded from iovs.arvojournals.org on 11/03/2026